Available online at www.sciencedirect.com
SCIENCE DIRECT
Icarus 181 (2006) 235–242
ICARUS
www.elsevier.com/locate/icarus

Sediment transport by liquid surficial flow: Application to Titan

Devon M. Burr [a,*], Joshua P. Emery [b], Ralph D. Lorenz [c], Geoffrey C. Collins [d], Paul A. Carling [e]

[a] *SETI Institute, 515 N. Whisman Rd., Mt. View, CA 94043, USA*
[b] *NASA Ames Research Center/SETI Institute, Mail Stop 245-6, Moffett Field, CA 94035, USA*
[c] *Lunar and Planetary Lab, University of Arizona, 1629 E. University Blvd., Tucson, AZ 85721, USA*
[d] *Physics and Astronomy Department, Wheaton College, Norton, MA 02766, USA*
[e] *School of Geography, Highfield University of Southampton, Southampton, SO17 1BJ, UK*

Received 17 June 2005; revised 12 November 2005

Available online 17 January 2006

Abstract

Sediment transport by surficial flow likely occurs on Titan. Titan is thought to have a volatile cycle, such as on Earth and likely in the past on Mars, which would entail surficial liquid flow. And surficial flow is implied in interpretations of Cassini–Hyugens data as showing fluvial channels, which would require sediment transport by surficial flow to form the observable features. We present calculations from basic hydraulic formulae of sediment entrainment and transport by surficial flow. First, we describe the conditions for (non-cohesive) sediment entrainment by grain size through use of the Shields' threshold curve. We then calculate settling velocities by grain size to describe the type of sediment transport—washload, suspended load, or bedload—that would follow entrainment. These calculations allow derivation of required flow depths for sediment transport by grain size over a given slope. A technique to estimate required flow velocities and unit discharges is also presented. We show the results of these calculations for organic and water ice sediment movement by liquid methane flow under Titan gravity. For comparative purposes, plots for movement of quartz sediment by water on Earth and basalt sediment by water on Mars are also included. These results indicate that (non-cohesive) material would move more easily on Titan than on Earth or Mars. Terrestrial field observations suggest that coarse grain transport is enhanced by hyperconcentration of fine-grained sediment; and the apparent availability of organic (fine grained) sediment on Titan, in conjunction with the possibility of convection-driven rainstorms, may lead to hyperconcentrated flows. Thus, significant sediment transport may occur on Titan during individual overland flow events.

Keywords: Titan; Mars, surface; Surfaces, planets; Satellites of Saturn; Surfaces, satellite

1. Introduction

Earth, Mars, and Titan are the three bodies in the Solar System currently inferred to show evidence for surficial liquid flow during volatile cycling. On Earth, this evidence appears as river channels and many other features in which liquid flow is active today. On Mars, similar evidence is visible as valley networks, intercrater deltas, and other possible aqueous flow features indicative of a past volatile cycle (e.g., Baker, 2001). On Titan, recent Cassini–Huygens results show dark, dendritic, fluviatile networks on bright, elevated surfaces (Porco et al., 2005; Elachi et al., 2005; Soderblom et al., 2005; Tomasko et al., 2005).

Volatile cycling and associated surficial flow on Earth or Mars involve or likely involved water. A volatile cycle on Titan likely involves hydrocarbons. At Titan's surface temperature (94 K) and pressure (1.44 bar), methane and ethane would be liquid (summarized in Lorenz et al., 2003). This fact has led to suggestions of hydrocarbon rains, lakes or seas, and possibly fluvial systems (Lunine et al., 1983; Ori et al., 1998). Ethane may be present in surficial bodies of water, but it is likely too involatile to be rapidly recycled by evaporation into Titan's atmosphere. Consequently, possible rainfall and rivers would be due to cycling of methane only (Lorenz and Lunine, 2005). Methane was first detected remotely in Titan's troposphere by Kuiper (1944). Samuelson et al. (1997) analyzed Voyager spec-

* Corresponding author.
E-mail address: dburr@seti.org (D.M. Burr).

0019-1035/$ – see front matter
doi:10.1016/j.icarus.2005.11.012

tra, indicating a near-surface methane mole fraction of ∼6% at low latitude, falling near-symmetrically to 2–3% at 60° latitude. Lemmon et al. (2002) suggested a low-latitude near-surface mole fraction of 3.8% using spatially-resolved near-infrared spectra acquired by the Hubble Space Telescope in 1997. The Huygens probe measured near-surface methane abundance at its low-latitude landing site of ∼5% by mass spectrometry (Niemann et al., 2005).

The expected liquid hydrocarbon seas are not apparent in the Cassini–Huygens optical or radar images acquired to date of Titan's surface (Turtle et al., 2005), but some features in these images are suggestive of fluvial systems (Elachi et al., 2005; Porco et al., 2005; Tomasko et al., 2005). Sediment entrainment, transport, and deposition by fluvial systems may have caused surficial modification over Titan's history, possibly accounting in part for the near absence of impact craters on Titan's surface (Porco et al., 2005). Fluvial systems on Earth entail overland flow in the interfluve areas and then channelized flow in the channels. Sediment entrained and transported by surficial flow on Earth and Mars is silicate material derived from the planets' crusts. Sediment on Titan is likely to be of two other types of material. One type would be water ice, derived from Titan's water ice outer crust (Stevenson, 1992; Lorenz and Lunine, 1996; Griffith et al., 2003). A second type would be organic material, which settles from the atmosphere after formation by photochemical reactions of hydrocarbons (Khare et al., 1978, 1984; Tran et al., 2003; Lorenz and Lunine, 2005).

Here we present calculations of sediment entrainment and transport by surficial flow. Hydraulic formulae are applied to estimate entrainment thresholds and settling velocities as a function of sediment grain size. The settling velocity estimates are then used to determine threshold frictional shear velocities for various types of transport. These calculations allow derivation of required depths of surficial flow for a given slope and sediment size. A technique to estimate mean flow velocities and unit discharges is also presented. We show results of these calculations for organic and water ice sediment entrainment and transport in liquid methane flow under Titan gravity. The results of most of these calculations are also presented for quartz sediment in water on Earth and basalt sediment in water on Mars to allow for comparison among the three bodies. The accuracy of these calculations depends upon the accuracy of the input parameter values refinement of values for materials on Titan will refine these results.

This paper addresses sediment entrainment and transport. Fluvial incision is addressed elsewhere (Soderblom et al., 2005; Collins, 2005).

2. Entrainment

Entrainment is the point at which the force or stress from a flowing fluid is sufficiently great as to move stationary sediment from the bed into transport. This point, also referred to as the threshold of sediment motion, is affected by numerous variables, including sediment size, shape, orientation, sorting and packing, fluid density and viscosity, and flow conditions. Because of this complexity and the seeming randomness of flow processes, the conditions for sediment entrainment are best treated as a stochastic process that is not understood deterministically but has been quantified empirically. This was first accomplished by Shields (1936), who showed a narrow range of threshold stresses necessary to entrain sediment of a given size. Subsequent workers have, for convenience, represented this narrow range of threshold stresses as a single line. Miller et al. (1977), for example, in reviewing available data for entrainment conditions under unidirectional flow, drew a single line for the entrainment threshold, and also extended the grain size range for which the Shields' curve is applicable. This line was subsequently used as the threshold curve for extraterrestrial (martian) sediment transport (Komar, 1980).

The Shield' curve is non-dimensional and applicable to a wide variety of flow circumstances, including extraterrestrial fluid flow (Miller and Komar, 1977). Shields (1936) combined the parameters of interest into a dimensionless threshold shear stress, θ_t, and the dimensionless boundary Reynolds number, Re_*. Reynolds number, Re, defines the laminar or turbulent character of the large scale flow. Boundary Reynolds number, Re_*, refers specifically to the liquid motion over the bed and describes the character of the flow at the liquid-solid interface. It can be stated as

$$Re_* = \frac{u_* d}{\upsilon} = \frac{u_* \rho d}{\eta}, \tag{1}$$

where u_* is the frictional shear velocity, d is the particle diameter (here, a proxy for roughness element height), υ is the kinematic viscosity $[L^2/T]$, ρ is the density of the liquid, and η is the dynamic viscosity $[M/LT]$, equal to $\rho\upsilon$. The dimensionless threshold shear stress for entrainment (the "Shields' criterion") is given by

$$\theta_t = \frac{\tau_t}{(\sigma-\rho)gd} = \frac{\rho u_*^2}{(\sigma-\rho)gd}, \tag{2}$$

where τ_t is the threshold shear stress exerted by the liquid flow, σ is the density of the sediment, and g is the acceleration of gravity.

Paphitis (2001) reviewed data from 36 investigations to derive an analytical expression for the Shields curve:

$$\theta_t = \frac{0.188}{1+Re_*} + 0.0475\left(1 - 0.699e^{-0.015Re_*}\right). \tag{3}$$

The entrainment data used in deriving this expression extend up to $Re_* \approx 10^5$; the correlation coefficient between this expression and the data is 0.813 (Paphitis, 2001). A plot of the Shields' curve derived from Eq. (3) is shown in Fig. 1. Higher entrainment thresholds at small particle sizes are due to hiding, cohesion among clay particles, and other factors. Higher entrainment thresholds at larger particle sizes are due to mass (weight). The values for the parameters used in this and subsequent calculations are found in Table 1. The Shields curves derived from each set of values, both terrestrial and extraterrestrial, are identical.

Both the dimensionless threshold shear stress, θ_t, and the dimensionless boundary Reynolds number, Re_*, relate to the fluid

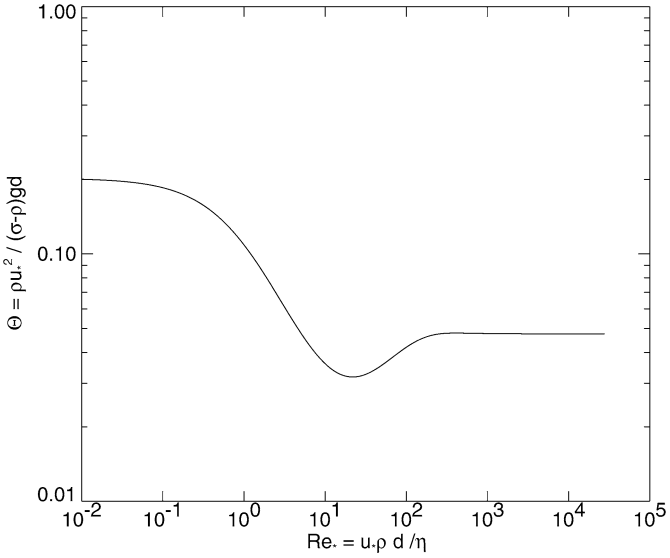

Fig. 1. Shields curve based on Eq. (3) (after Paphitis, 2001).

and sediment properties and can be stated in terms of u_* and d (Eqs. (1) and (2)). Thus, for a given fluid and sediment, Eq. (3) can be solved for u_* for a range of diameters. That solution provides the minimum shear stress required to entrain sediment in terms of (dimensional) grain size, and is shown as the threshold curves between no motion and bedload in Figs. 3 and 4.

3. Transport

Once entrained, sediment may be transported by flowing liquid in three ways. Coarse sediment moves as 'bedload' by sliding, rolling, or saltating on the bed. Finer sediment moves as 'suspended load,' concentrated near the bed but found throughout the liquid column due to vertical currents in the flow. 'Washload,' composed of the finest sediment, is uniformly distributed in the liquid column above the bed. Rouse (1937) and subsequent workers (e.g., Bagnold, 1966) have distinguished these three categories by rationing the settling velocity of the particle (its rate of fall under quiescent conditions) to the flow frictional shear velocity (a proxy for the turbulence acting to suspend particles):

$$k = \frac{w_s}{u_*}, \tag{4}$$

where k is the threshold ratio for distinguishing between transport categories, and w_s is the settling velocity.

Values for the two thresholds—between bedload and suspended load, and between suspended load and washload—have been estimated from experiments. Studies place the value of k for the bedload to suspended load transition at 1.00–1.79 (summarized by Komar, 1980). The variation is due both to differences in threshold criteria used by different observers and to the somewhat arbitrary nature of drawing a sharp boundary in a continuum between transport classes (e.g., grains in bedload transport begin to saltate increasingly long distances before transitioning to suspension). The k values for the suspended to washload transition have generally been given less attention, and the physical processes responsible for holding material in washload (e.g., 'autosuspension'; Bagnold, 1962; Nordin, 1963) are less well understood. Consequently, a literature review finds these k values to have a slightly wider range proportionately—from 0.05 to 0.13—than that for the bedload-suspended load threshold (summarized by Komar, 1980). Despite the artificiality of drawing a single boundary for a continuum process, reported values for each threshold fall within a factor of 2–3 of one another, and the ranges of values for the two different thresholds are quite distinct. For this work, 1.25 is used as the threshold value between bedload and suspended load (after Komar, 1980) and 0.075 is used as the k value between suspended and washload.

Calculating settling velocities of sediment in liquid is accomplished using empirical fits to settling velocity data, as presented first by Turton and Clark (1987) and re-evaluated for non-Newtonian flows by Kelessidis (2004). These data cover the entire laminar regime for the particle, i.e., where particle Reynolds number, Re_p, is less than $\sim 10^5$ (Graf, 1971; Turcotte and Schubert, 1982, pp. 266–267). In the same way that boundary Reynolds number, Re_*, describes flow conditions at the bed, particle Reynolds number, Re_p, describes flow conditions around a settling particle. It is given by

$$Re_p = \frac{w_s \rho d}{\eta}. \tag{5}$$

The Stokes law of settling gives the particle settling velocity as a function of particle and fluid properties and gravity, namely:

$$w_s = \frac{d^2}{18}\frac{g(\sigma - \rho)}{\eta}. \tag{6}$$

Table 1
Parameter values used for comparative modeling of sediment entrainment and transport by liquid overland flow on Earth, Mars, and Titan

	Earth	Mars	Titan
Sediment	Quartz	Basalt	H_2O ice
σ = particle density	$\sigma = 2650$ kg/m^3	$\sigma = 2900$ kg/m^3	$\sigma = 992$ kg/m^3
			Organics
			$\sigma = 1500$ kg/m^3
Fluid	Water	Water	CH_4/N_2
ρ = fluid density	$\rho = 1000$ kg/m^3	$\rho = 1000$ kg/m^3	$\rho = 450$ kg/m^3
η = dynamic viscosity	$\eta = 1 \times 10^{-3}$ Pa s	$\eta = 1 \times 10^{-3}$ Pa s	$\eta = 2 \times 10^{-4}$ Pa s
Gravity	9.8 m/s^2	3.7 m/s^2	1.35 m/s^2

Titan fluid density and viscosity values taken from Lorenz et al. (2003); organic density from Khare et al. (1994), but values down to ~400 kg/m^3 (e.g., Bott, 1986) are possible.

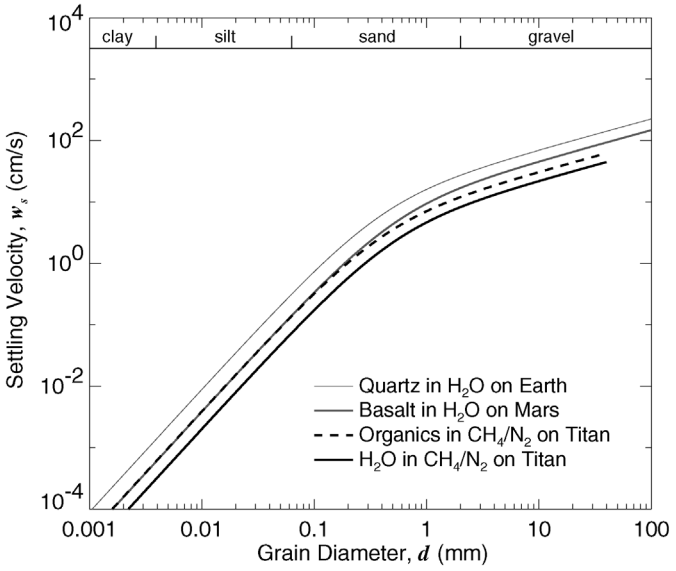

Fig. 2. Settling curves for quartz on Earth, basalt on Mars, and organic material and ice on Titan. The extents of the plots indicate the applicable grain sizes.

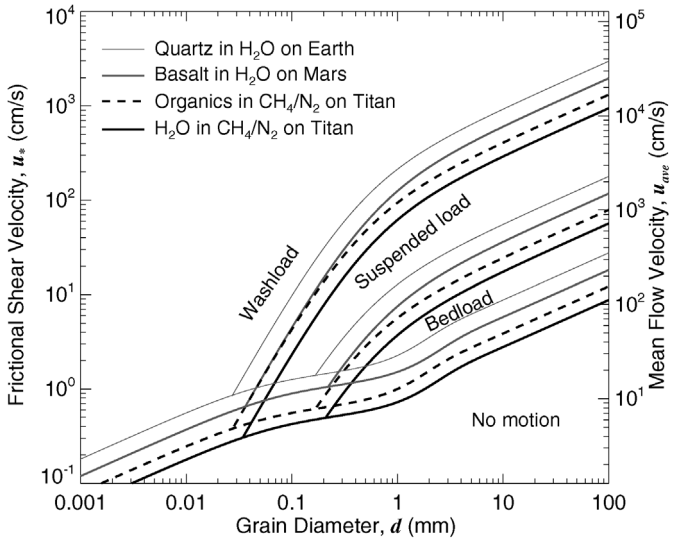

Fig. 3. Fields of transport categories for quartz on Earth, basalt on Mars, and organic material and water ice on Titan. The threshold k value used here for the bedload-suspended load transition is 1.25; the threshold k value used here for the suspended-washload transition is 0.075. Mean flow velocity, u_{ave}, is for a gravel bed river with a D_{84} of 256 mm.

Strictly, the Stokes equation is applicable only the lowest range of the laminar regime, where $Re_p < 1$; therefore, its use by Burr et al. (2005) to calculate settling velocities for the entire laminar regime for the particle was a simplification and is superseded by this more comprehensive work.

Dimensionless diameter and settling velocity for spherical particles are defined by

$$d_* = d\left[\frac{g\rho(\sigma-\rho)}{\eta^2}\right]^{1/3} \tag{7}$$

and

$$w_{s*} = w_s\left[\frac{\rho^2}{g\eta(\sigma-\rho)}\right]^{1/3}, \tag{8}$$

respectively. Using Stokes law (6) for the low Reynolds number range and a constant drag coefficient for the high Reynolds number range (see, e.g., Turcotte and Schubert, 1982, Fig. 6-32), these dimensionless quantities can be related by the expression

$$w_{s*} = \left[\left(\frac{18}{d_*^2}\right)^{K_2} + \left(\frac{3}{4}\frac{K_1}{d_*}\right)^{K_2/2}\right]^{-1/K_2}, \tag{9}$$

where $K_1 = 0.428$ and $K_2 = 0.824$ were determined empirically (Turton and Clark, 1987; Kelessidis, 2004). For a given particle size, these equations can be evaluated to find the settling velocity, w_s, for $Re_p \leqslant 10^5$ (that is, within the laminar regime). These results are presented in Fig. 2. The terrestrial and martian curves shown on Fig. 2 adequately reproduce the terrestrial and martian curves of Komar (1980, his Fig. 1), which were derived from a graphical presentation of drag coefficient curves. Equation (9) is valid to a maximum grain size as determined for $Re_p \sim 10^5$ and the relation between w_s and d given in Eqs. (7)–(9). On Earth and Mars, this maximum grain size equals 100 mm; on Titan, it equals ∼44 mm (Fig. 2). For minimum grain sizes, the provided plots encompass clay-sized material. However, particle cohesion, flocculation, and other interactions among clay-sized particles have a strong influence on entrainment and transport of terrestrial clayey sediments. The cohesion and other possible interactions of Titan organic material are unknown and require further investigation.

Using Eq. (4), the settling, or terminal, velocity may then be divided by the two threshold ratio values, k, for bed-suspended load and suspended-wash load to find the frictional shear velocities that distinguish among the three transport regimes as a function of sediment size. The results of these calculations are presented in Fig. 3. Also included in Fig. 3 are the bedload threshold curves calculated as described in Section 2. The intersection of the bedload threshold (or entrainment) curves with the suspended load or wash load curves indicates that the material, when entrained, moves directly into suspended load or washload transport.

Some observations may be made from these plots. Both the settling velocity curves and the frictional velocity curves show a bend near a grain diameter of ∼0.4 mm, where the more steeply sloping lower portion flattens into a more shallowly sloping upper portion (Figs. 2 and 3). This bend marks the transition from Stokes flow (lower portion) to non-Stokes flow (upper portion). These two types of laminar flow are expressed in the first and second terms of Eq. (9) (Turton and Clark, 1987; Kelessidis, 2004). Setting the second term of Eq. (9) equal to zero and solving for the settling velocity gives the Stokes equation (Eq. (6)). In the Stokes regime, settling velocity is proportional to the square of the grain diameter and to the gravitational acceleration and inversely proportional to viscosity ('viscous resistance dominates'). Setting the first term of Eq. (8) equal to zero and solving for the settling velocity gives

$$w_s = \left[\frac{4d}{3K_1}\frac{g(\sigma-\rho)}{\rho}\right]^{1/2}. \tag{10}$$

This shows that in the non-Stokes regime, settling velocity is proportional to the square root of both the grain diameter and the gravitational acceleration, but that viscosity is not a factor in this regime ('inertial forces dominate'). These and other differences between the equations for Stokes and non-Stokes flow (Eqs. (6) and (10)) produce the two different slopes of the settling and frictional velocity curves.

A second observation that can be made from the frictional shear velocity curves is the convergence of the washload threshold curves for basalt transport in water on Mars and organic sediment transport in liquid methane on Titan (Fig. 3). This convergence near ~0.070 mm shows that the combination of parameters in Eq. (8) produces very similar values for these two situations. Very fine or finer basaltic sand in water on Mars should behave like similarly-sized organic sediment in liquid methane on Titan.

Fig. 3 also shows that for a given frictional shear velocity, similar or larger grains can be transported by liquid flow on Titan than on Mars or on Earth. Or, stated conversely, slower flow is required to transport material on Titan than on Mars or Earth. These calculations apply only to the ability of the liquid to transport sediment of a given size (the 'competence'); the actual transport may be limited by the availability of sediment and the amount of liquid flow.

According to these calculations, water ice sediment is transported more easily than organic sediment on Titan. This is a result of the density that we have used for organic material (1500 kg/m^3; Khare et al., 1994; Moroz et al., 1998; Imanaka et al., in preparation) being higher than that of water ice. However, the density of organics on Titan is uncertain. Particles settling from the atmosphere could have densities as low as ~400 kg/m^3 (Bott, 1986), lower than expected densities of surface liquid hydrocarbons (Lunine, 1993). In this case, the particles would float, an explanation suggested for the lack of detection of liquid hydrocarbons by the Cassini Titan Radar Mapper (Elachi et al., 2005). If organic particles float on Titan liquid hydrocarbons, these calculations for organic sediment transport would be irrelevant. Less extreme values of organic material density, if still greater than the density of liquid methane but less than that of water ice, would shift the organic curves below the water ice curves in Fig. 3.

4. Overland flow depths and possible enhancement of sediment transport

For uniform or near-uniform flow, the relation between frictional shear velocity and flow depth is given by

$$u_* = (ghS)^{1/2}, \tag{11}$$

where h is the flow depth and S is the bed slope. In conjunction with Eq. (4), this relationship can be used to calculate the minimum flow depth necessary to obtain shear velocities required to transport sediment as bedload, suspended load, and washload. This approach can then be used to estimate flow depths required to transport sediment of a given size over slopes of a known value.

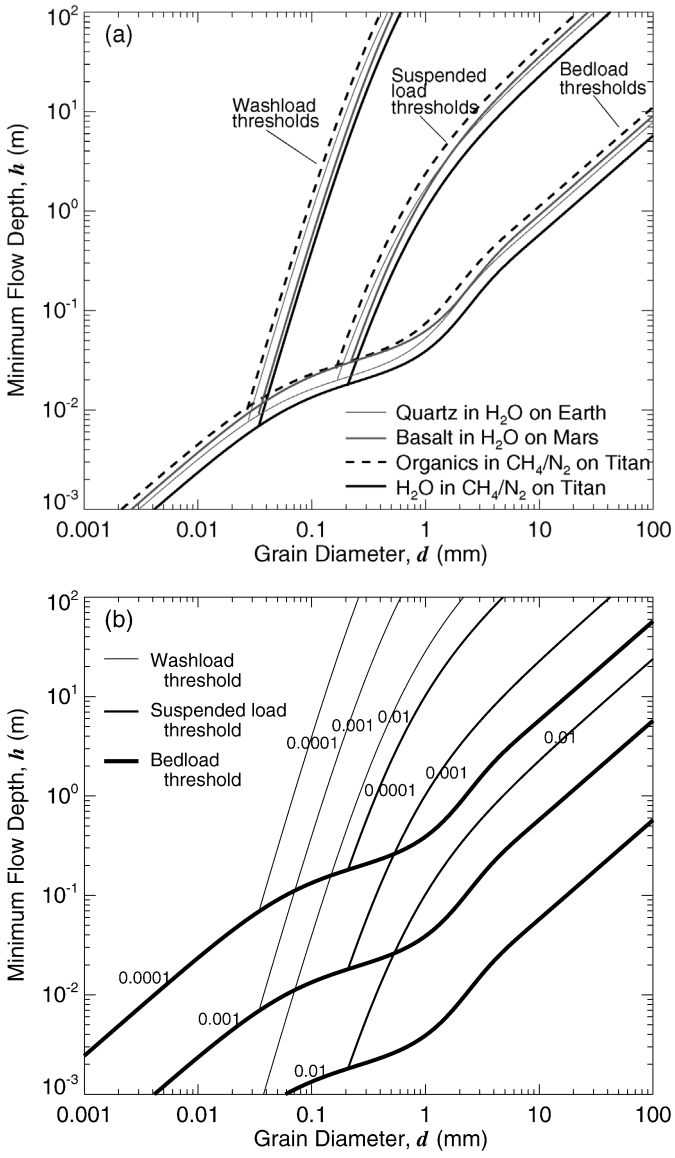

Fig. 4. (a) Minimum flow depths required to carry quartz on Earth, basalt on Mars, and organic material and ice on Titan over a slope of 0.001. (b) Minimum flow depths required to carry ice on Titan for three different slopes of 0.0001, 0.001, and 0.01. Type of threshold is indicated by line thickness; slope is indicated by numbers on lines. For comparison, the Mississippi River has an overall slope of roughly 0.0001 (Jordon, 1965), and the Channeled Scabland catastrophic flood terrain in Washington state, USA, has an overall slope of roughly 0.03 (Baker, 1973).

Fig. 4 shows sample results for a range of conditions and slopes. Fig. 4a indicates that for all three bodies, 10-μm-sized sediment (if non-cohesive) is small enough that virtually any flow will entrain it. Fig. 4b gives an idea of the variation in threshold curves induced by variation in slope.

Fig. 4a indicates that less liquid is required to transport material of a given grain size on Titan than on either Earth or Mars. If significant organic material precipitates onto the surface (Khare et al., 1978, 1994; Lunine, 1993), it may further enhance sediment transport on Titan. Entrainment of more than 40% sediment by weight converts a fluvial flow into a hyperconcentrated flow, such as often occurs in the American southwest

during convection-driven rainstorms (Beverage and Culbertson, 1964). Hyperconcentration due to entrainment of finer grained sediment reduces the settling velocities of coarser grained sediment. This reduction in settling velocity results from the increases in both effective viscosity of the flowing material and effective buoyancy of the particle (Beverage and Culbertson, 1964). The increased effective viscosity of hyperconcentrated flow may reduce the turbulence tending to keep particles in suspension, but this effect is thought to be less significant than the decrease in settling velocity (see, e.g., Beverage and Culbertson, 1964, pp. 126–128). As a result, coarser material which in clear liquid flow would move as bedload can in hyperconcentrated flow move as suspended load or washload (Nordin, 1963; Komar, 1980). In comparison to bedload, suspended load and washload both move quickly, i.e., near or at the rate of the overland liquid flow. So availability of finer-grained sediment tends to increase the rate of coarser grained sediment transport. If organic (i.e., fine grained) material (Elachi et al., 2005) combine with possible methane rainstorms (Lorenz et al., 2005) to produce hyperconcentrated flows on Titan, the transport of coarser, water ice sediment would be enhanced. For that reason, these calculations for water ice sediment transport on Titan are considered conservative: methane rainstorms on organic-laden surfaces may produce hyperconcentrated flow, leading to more coarse-grained sediment transport than estimated with these clear-liquid flow calculations.

5. Minimum flow velocity and unit discharge required to transport sediment

To convert frictional shear velocities into true flow velocities, a measure of the resistance of the bed on the flowing liquid is required. Some frictional coefficients, such as Manning's n or Chezy's C, are dimensional and non-physical—for example, Manning's n has dimensions of $T/L^{1/3}$—and they implicitly account for (terrestrial) gravity. Thus their application to extraterrestrial flow has been somewhat ad hoc (see Wilson et al., 2004, for discussion).

As first discussed by Komar (1979), the Darcy–Weisbach equation explicitly accounts for gravity and uses a non-dimensional frictional coefficient, f_c. Wilson et al. (2004) summarized and simplified the work of Bathurst (1993) in presenting Darcy–Weisbach formulae for channelized flow under martian conditions. Though derived from and previously applied to water, these formulae are held to be applicable to 'any low viscosity liquid' (Wilson et al., 2004). Formulae 13 and 14 from Wilson et al. (2004) provide estimates of the Darcy–Weisbach frictional coefficient for flow over a sand bed and a gravel bed, respectively,

$$(8/f_c)^{1/2} = 8.46(R/D_{50})^{0.1005} \tag{12}$$

and

$$(8/f_c)^{1/2} = 5.75\log_{10}(R/D_{84}) + 3.514, \tag{13}$$

where R is the hydraulic radius, which for natural, broad terrestrial channels can be approximated by the channel depth, and D_{50} and D_{84} are the bed clast size for which 50% and 84% of the clasts are finer, respectively. (According to the modified Wentworth scale, sand size sediment ranges for 0.0625–2 mm; gravel size sediment ranges from 2–265 mm.) As their incorporation into these frictional coefficients indicates, these clast sizes are determinants for the amount of flow resistance exerted by the bed; they are not necessarily the size of material in transport, which of course is dependent on flow conditions.

The quantity $f_c/8$ is equivalent to the generic dimensionless friction coefficient, C, of Komar, 1979 (p. 178) that relates u_* to u_{ave}, the average true flow velocity (Komar, 1980; compare his Eq. (6) to his Eq. (8) to see that the exponent in Eq. (8) is missing a negative sign). From that presentation, the quantity $(8/f_c)^{1/2}$ can be seen to be a direct proportionality constant between u_* and u_{ave}:

$$u_{\text{ave}} = (8/f_c)^{1/2}u_*. \tag{14}$$

For a sand bed river with a D_{50} of 0.0625 mm, f_c is ~0.01 and the quantity $(8/f_c)^{1/2}$ is ~28.2. For a gravel bed river with a D_{84} of 256 mm, f_c is ~0.05 and the quantity $(8/f_c)^{1/2}$ is ~12.7. These example sediment sizes are chosen to maximize the difference between the resultant values. As these examples show, the differences in results are still within a factor of a few. Fig. 3 gives an ordinate axis scaled by a factor of 12.7 for u_{ave} values derived from u_* values for the gravel bed example with $D_{84} = 256$ mm. Because these u_* values are thresholds for transport, the example associated u_{ave} values as indicated by the right ordinate axis are also minima for the designated categories of transport.

The flow velocity can be used in conjunction with the flow depth to estimate the mass flow rate per unit area, or unit discharge $[L^2/T]$, required to transport sediment. A rearrangement of Eq. (11) to solve for depth shows that $h = (u_*)^2/gS$. Replacing u_* with the equivalent expression using u_{ave} gives

$$h = \frac{u_{\text{ave}}^2(f_c/8)}{gS}. \tag{15}$$

Unit discharge is the product of flow velocity and depth, such that

$$u_{\text{ave}}h = \frac{u_{\text{ave}}^3(f_c/8)}{gS} = \frac{u_*^3(8/f_c)^{1/2}}{gS}. \tag{16}$$

The results of this calculation vary with varying estimates of f_c (which varies depending on the type of bed, sand or gravel, and the grain size distribution, as represented by the values for D_{50} and/or D_{84}). For the two extreme cases given above, i.e., a sand bed where $D_{50} = 0.0625$ mm and a gravel bed where $D_{85} = 256$ mm, the results are plotted in Fig. 5.

Refinement of these calculations with Cassini–Huygens data from Titan or from other work will improve them, and illustrate their full utility. Data from Cassini's Titan Radar Mapper (Elachi et al., 2005) will provide slope values to determine if the simplifications presented by Wilson et al. (2004) and used here, including the assumption of slopes between 0.001 and 0.003, are appropriate for use on Titan. Sediment size distributions from analysis of Cassini–Huygens data (e.g., Tomasko et al., 2005) will allow assessment of whether a sand or gravel bed equation is appropriate as well as estimation of D_{50} and/or

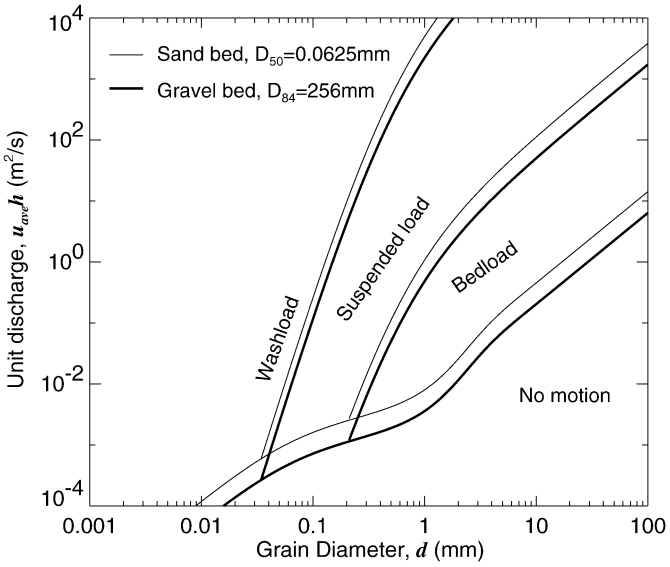

Fig. 5. Example minimum unit discharges necessary to entrain and transport sediment. Grain sizes are selected to give extreme (maximum and minimum) results.

D_{84}, as necessary. Estimates of unit discharge can be compared with estimated methane rainfall rates (Lorenz, 2000; Lorenz et al., 2005) needed to transport material to determine likely sediment transport rates and amounts.

6. Conclusions

As shown by Figs. 2–4, the required conditions for sediment entrainment and transport by liquid methane flow on Titan are within a factor of a few (for organic material) or several (for water ice) for sediment entrainment and transport by liquid water flow on Earth or Mars. That is, the required flow velocity (Fig. 3) and flow depth (Fig. 4a) are generally lower for Titan than for Earth or Mars, although the required flow depth for high-density organic material on Titan is higher (Fig. 4a). This result suggests that similar overland flow processes occur on Titan as occur on Earth and apparently occurred on Mars. As fluvial channels require sediment entrainment and transport for their formation, the data in Figs. 2–4 are consistent with the suggestion that dark curvilinear features on Titan are fluvial channels (Porco et al., 2005; Elachi et al., 2005), entailing surficial overland and channelized overland flow.

This work presents simple methods to estimate the hydraulic (methan-aulic?) parameters—namely, flow depth, velocity, and unit discharge—required to entrain and to transport sediment by surficial flow. Use of these methods with slope and sediment size data from the Cassini–Huygens mission should allow accurate derivation of flow conditions on Titan. This work is considered conservative, however, inasmuch as fine-grained sediment would tend to increase the concentration of the flow, decreasing sediment settling velocities and increasing coarse grain transport. The availability of organic (fine grained) sediment on Titan (Elachi et al., 2005), in conjunction with the possibility of convention-driven rainstorms (Lorenz et al., 2005), suggests that hyperconcentrated flows may be common, leading to enhanced transport of coarser grained (water ice) sediment. In comparison to Earth and Mars, greater sediment transport may occur on Titan during individual, hyperconcentrated flow events. Sediment movement could thus be a factor in Titan resurfacing and the lack of apparent craters (Porco et al., 2005).

Acknowledgments

We thank Gian Gabriele Ori and an anonymous reviewer for helpful comments.

References

Bagnold, R.A., 1962. Auto-suspension of transported sediment: Turbidity currents. Proc. R. Soc. London Ser. A 265, 315–319.
Bagnold, R.A., 1966. An approach to the sediment transport problem from general physics. U.S. Geol. Surv. Prof. Paper 422-I.
Baker, V.R., 1973. Paleohydrology and sedimentology of Lake Missoula flooding in eastern Washington. Geol. Soc. Am. Spec. Paper 144. 79 pp.
Baker, V.R., 2001. Water and the martian landscape. Nature 412, 228–236.
Bathurst, J.C., 1993. Flow resistance through the channel network. In: Beven, K., Kirby, M.J. (Eds.), Channel Network Hydrology. Wiley, New York, pp. 69–98.
Beverage, J.P., Culbertson, J.K., 1964. Hyperconcentrations of suspended sediment. J. Hydraul. Div., Proc. Am. Soc. Civil Eng. HY6 (Nov.), 117–128.
Bott, D., 1986. Structural basis for semiconducting and metallic polymers. In: Skotheim, T. (Ed.), Handbook of Conducting Polymers, vol. 2. Dekker, New York, pp. 1191–1232.
Burr, D.M., Emery, J.P., Lorenz, R.D., 2005. Theoretical calculations on sediment transport on Titan, and the possible production of streamlined forms. Lunar Planet. Sci. XXXVI. Abstract 2044.
Collins, G.C., 2005. Relative rates of fluvial bedrock incision on Titan. Geophys. Res. Lett. 32 (22), doi:10.1029/2005GL024551. L22202.
Elachi, C., and 34 colleagues, 2005. Cassini radar views the surface of Titan. Science 308, 970–974.
Graf, W.H., 1971. Hydraulics of Sediment Transport. McGraw-Hill, New York.
Griffith, C.A., Owen, T., Geballe, T.R., Rayner, J., Rannou, P., 2003. Evidence for exposure of water ice on Titan's surface. Science 300, 628–630.
Jordon, P.R., 1965. Fluvial sediment of the Mississippi River at St. Louis, Missouri. U.S. Geol. Surv. Water-Supply Paper 1802.
Kelessidis, V.C., 2004. An explicit equation for the terminal velocity of solid spheres falling in pseudoplastic liquids. Chem. Eng. Sci. 59, 4435–4445.
Khare, B.N., Sagan, C., Bandurski, E.L., Nagy, B., 1978. Ultraviolet-photoproduced organic solids synthesized under simulated jovian conditions: Molecular analysis. Science 1999, 1199–1201.
Khare, B.N., Sagan, C., Arakawa, E.T., Suits, F., Callcott, T.A., Williams, M.W., 1984. Optical constants of organic tholins produced in a simulated titanian atmosphere—From soft X-ray to microwave frequencies. Icarus 60, 127–137.
Khare, B.N., Sagan, C., Thompson, W.R., Arakawa, E.T., Meisse, C., Tuminello, P.S., 1994. Optical properties of poly-HCN and their astronomical applications. Can. J. Chem. 72, 678–694.
Komar, P.D., 1979. Comparisons of the hydraulic of water flow in martian outflow channels with flows of similar scale on Earth. Icarus 37, 156–181.
Komar, P.D., 1980. Modes of sediment transport in channelized water flows with ramifications to the erosion of the martian outflow channels. Icarus 42, 317–329.
Kuiper, G.P., 1944. Titan: A satellite with an atmosphere. Astrophys. J. 100, 378–383.
Lemmon, M.T., Smith, P.H., Lorenz, R.D., 2002. Methane abundance on Titan, measured by the Space Telescope Imaging Spectrograph. Icarus 160, 375–385.
Lorenz, R.D., 2000. The weather on Titan. Science 290, 467–468.
Lorenz, R.D., Lunine, J.I., 1996. Erosion on Titan: Past and present. Icarus 122, 79–91.

Lorenz, R.D., Lunine, J.I., 2005. Titan's surface before Cassini. Planet. Space Sci. 53, 557–576.

Lorenz, R.D., Kraal, E., Asphaug, E., Thomson, R.E., 2003. The seas of Titan. Eos 84 (14), 125, 131–132.

Lorenz, R.D., A Griffith, C., Lunine, J.I., McKay, C.P., Renno, N.O., 2005. Convective plumes and the scarcity of clouds on Titan. Geophys. Res. Lett. 32. L01201.

Lunine, J.I., 1993. Does Titan have an ocean? A recent review of current understanding of Titan's surface. Rev. Geophys. 31, 133–149.

Lunine, J.I., Stevenson, D.J., Yung, Y.L., 1983. Ethane ocean on Titan. Science 222, 1229–1230.

Miller, M.C., Komar, P.D., 1977. The development of sediment threshold curves for unusual environments (Mars) and for inadequately studied material (foram sands). Sedimentology 24, 709–721.

Miller, M.C., McCave, I.N., Komar, P.D., 1977. Threshold of sediment motion under unidirectional currents. Sedimentology 24, 507–527.

Moroz, L.V., Arnold, G., Korochantsev, A.V., Wäsch, R., 1998. Natural solid bitumens as possible analogs for cometary and asteroid organics. 1. Reflectance spectroscopy of pure bitumens. Icarus 134, 253–268.

Niemann, H.B., and 17 colleagues, 2005. The abundances of constituents of Titan's atmosphere from the GCMS instrument on the Huygens probe. Nature 438, 779–784.

Nordin, C.F., 1963. Sedimentary Transport in Alluvial Channels: A preliminary study of sediment transport parameters, Rio Puerco near Bernardo, New Mexico. U.S. Geological Prof. Paper 462-C.

Ori, G.G., Marinangeli, L., Baliva, A., Bressan, M., Strom, R.G., 1998. Fluid dynamics of liquids on Titan's surface. Planet. Space Sci. 46 (9/10), 1417–1421.

Paphitis, D., 2001. Sediment movement under unidirectional flows: An assessment of empirical threshold curves. Coast. Eng. 43, 227–245.

Porco, C.C., and 35 colleagues, 2005. Imaging of Titan from the Cassini spacecraft. Nature 434, 159–168.

Rouse, H., 1937. Modern conceptions of the mechanics of turbulence. Trans. Am. Soc. Civ. Eng. 102, 463–543.

Samuelson, R.E., Nath, N.R., Borysow, A., 1997. Gaseous abundances and methane supersaturation in Titan's troposphere. Planet. Space Sci. 45, 959–980.

Shields, A., 1936. Application of similarity principles and turbulence research to bed-load movement. In: Mitteilungen der Preussischen Versuchsanstalt für Wasserbau und Schiffbau, Berlin. California Inst. Tech., W.M. Keck Lab. of Hydraulics and Water Resources. Rept. No. 167. Ott, W.P. and Van Uchelen, J.C. (translators).

Soderblom, L., and 40 colleagues, 2005. Titan's surface as viewed from the Huygens Probe by the Descent Imager/Spectral Radiometer. GSA Abstracts with Programs 37 (7), 237. Paper No. 102-9.

Stevenson, D.J., 1992. The interior of Titan. In: Proceedings of the Symposium on Titan. In: ESA SP-338. ESA, Noordwijk, The Netherlands, pp. 29–33.

Tomasko, M.G., and 39 colleagues, 2005. Rain, winds, and haze during the Huygens probe's descent to Titan's surface. Nature 438, 765–778.

Tran, B.N., Jones, J.C., Ferris, J.P., Persans, P.D., Chera, J.J., 2003. Simulation of Titan haze formation using a photochemical flow reactor: The optical constants of the polymer. Icarus 165, 379–390.

Turcotte, D.L., Schubert, G., 1982. Geodynamics: Applications of Continuum Physics to Geological Problems. Wiley, New York. 450 pp.

Turtle, E.P., Dawson, D.D., Fussner, S., Hardegree-Ullman, E., McEwen, A.S., Perry, J.E., Porco, C.C., West, R.A., the Cassini ISS team, 2005. Liquid hydrocarbons on Titan's surface? How Cassini ISS observations fit into the story (so far). Lunar Planet. Sci. XXXVI. Abstract 2311.

Turton, R., Clark, N.N., 1987. An explicit relationship to predict spherical particular terminal velocity. Powder Technol. 53, 127–129.

Wilson, L., Ghatan, G.J., Head, J.W., Mitchell, K.L., 2004. Mars outflow channels: A reappraisal of the estimation of water flow velocities from water depths, regional slopes, and channel floor properties. J. Geophys. Res. 109, doi:10.1029/2004JE002281. E09003.